A generalized numerical approach to steady-state enzyme kinetics: Applications to protein kinase inhibition

Petr Kuzmič

BioKin Ltd., 15 Main Street Suite 232, Watertown, MA 02472, USA

ARTICLE INFO

ABSTRACT

A generalized numerical treatment of steady-state enzyme kinetics is presented. This new approach relies on automatic computer derivation of the underlying mathematical model (a system of simultaneous nonlinear algebraic equations) from a symbolic representation of the reaction mechanism (a system of biochemical equations) provided by the researcher. The method allows experimental biochemists to analyze initial-rate enzyme kinetic data, under the steady-state approximation, without having to use any mathematical equations. An illustrative example is based on the inhibition kinetics of $p56^{lck}$ kinase by an ATP competitive inhibitor. A computer implementation of the new method, in the modified software package DYNAFIT [Kuzmič, P. (1996) *Anal. Biochem.* 237, 260–273], is freely available to all academic researchers.

© 2009 Published by Elsevier B.V.

1. Introduction

Enzyme kinetics—together with structural studies (X-ray crystallography, NMR spectroscopy, molecular modeling) and biological assays—is one of several important experimental methods employed for the study of inhibitors of protein kinases. One serious disadvantage of the formal kinetic analysis is its mathematical complexity. Even in the absence of inhibitors, a traditional algebraic rate equation for a protein kinase derived under the steady-state approximation [1] might be exceedingly complex, while still being applicable only to certain special experimental situations. Specifically, under the traditional algebraic formalism we must assume that the enzyme concentration is infinitely smaller than the concentrations of all substrates.

The mathematical complexity substantially increases when inhibitors are considered, in addition to substrates, and a new fundamental problem emerges in the case of "tight binding" inhibitors [2]. The traditional algebraic formalism for initial rate enzyme kinetics is unsuitable for handling tight binding inhibitors, except in the special case where the inhibitor forms a 1:1 complex with the enzyme [2]. For example, if a hypothetical tight binding inhibitor were to bind simultaneously (and "tightly") both to the active site and to an allosteric site, the resulting algebraic rate equation would be so complex as to be practically unusable.

To allow the study of "tight-binding" enzyme inhibitors without any restrictions being placed on the number of binding sites, or on any other particular characteristics of the molecular mechanism, we have previously described [3] a general numerical approach to initial-rate enzyme kinetics under the rapid-equilibrium approximation [1]. The two major advantages of this general numerical approach are convenience and generality.

The iterative numerical approach is indeed convenient, because it allows the researcher to specify the postulated biochemical mechanism without the use of any mathematical equations. Instead, we can supply the description of the biochemical system in the familiar biochemical notation, using stoichiometric equations (e.g., $E + A <==> E.S -> E + P$ for the Michaelis–Menten mechanism). A suitable computer algorithm [4,5] then automatically translates the biochemical notation into the corresponding mathematical structures.

The second major advantage of the general numerical approach [3] is that it applies not only to "classical" inhibition, where the concentrations of all inhibitors are assumed to be infinitely larger than the concentration of the enzyme, but also to "tight binding" systems, where the concentrations of all components can be in principle comparable in magnitude. This opens the possibility of studying the detailed kinetic behavior of therapeutic enzyme inhibitors, which typically bind very tightly to the target enzyme.

The general numerical approach as previously described [3] applies only to enzyme–inhibitor systems under the rapid-equilibrium approximation, where we assume that the binding and dissociation of all substrates and other ligands is infinitely rapid, when compared

with the rate of the chemical step (in the case of protein kinases, the phosphoryl transfer step). However, there is no reason to believe that the rapid-equilibrium assumption is valid in every protein kinase assay. For example, Keshwami and Harris [6] recently established that, at least in the specific case of the fully activated S6K1 protein kinase, ADP release is rate limiting.

In this paper, we describe an extension and further generalization of the previously described numerical treatment of initial-rate enzyme kinetics [3]. Here we remove the simplifying rapid-equilibrium approximation, and invoke instead the more general steady-state approximation. Thus, in the specific case of protein kinases, we no longer assume that the phosphoryl transfer step is strictly rate limiting.

2. Theory

2.1. Definitions and assumptions

Let n_O be the number of reactants appearing in the overall reaction described by the stoichiometric vector **s** (see below for an illustrative example of all matrices and vectors utilized in this study). Unlike in the classical algebraic formalism [1], we do not assume that overall reactants are present at concentrations very much higher than the enzyme.

Let n_M be the number of modifiers, such as inhibitors or activators. For example, we could have a mixture of two inhibitors (perhaps involving a prodrug, a stereoisomer, or a metabolite), either of which can be "tight binding" [2], and which can bind to any number of enzyme forms with any stoichiometry. With only one inhibitor being present, and no activators, we typically have $n_M = 1$.

Let n_E be the number of elements, or component species [7], that appear in the reaction mechanism. These include the overall reactants, the modifiers, and the enzyme catalyst. Thus, $n_E = n_O + n_M + 1$.

Let n_C be the number of distinct enzyme complexes that appear in the molecular mechanism.

Let n_S be the total number of molecular species participating in the mechanism. Thus, $n_S = n_E + n_C$.

Let n_R be the number of elementary or microscopic reactions that appear in the overall molecular mechanism. Thus, the stoichiometric matrix [3,7], **S**, has n_R rows and n_S columns.

Let the stoichiometric matrix **S** be ordered such that the first n_E columns are assigned to the component species (so that the last n_C columns are assigned to enzyme complexes). The molecular species are ordered identically in the steady-state concentration vector, $\tilde{\mathbf{c}}$.

Let **T** be the truncated stoichiometric matrix, taken as the last n_C columns of the complete stoichiometric matrix **S**. Thus, the truncated matrix **T** describes the interactions of the n_C enzyme complexes.

Let **F** be a formula matrix [3,7] with n_S columns and n_E rows, expressing the composition of all molecular complexes in terms of components. The mass balance equations for component species can be written as shown in Eq. (1), where the left-hand side is an n_E-vector and $\mathbf{c}^{(t)}$ is a vector of total or analytic concentrations.

$$0 = \mathbf{F}\tilde{\mathbf{c}} - \mathbf{c}^{(t)} \tag{1}$$

Let **v** be the n_R-vector of elementary or microscopic rate terms defined, in terms of the stoichiometric matrix **S**, as shown in Eq. (2) where k_i ($i = 1, ..., n_R$) are microscopic rate constants, and δ_j is defined by Eq. (3).

$$v_i = k_i \prod_{j=1}^{n_S} c_j^{-\delta_j S_{i,j}}; i = 1, \cdots, n_R \tag{2}$$

$$\delta_j = \begin{cases} 1 \text{ if } S_{i,j} < 0 \\ 0 \text{ if } S_{i,j} \geq 0 \end{cases} \tag{3}$$

Let us now formally invoke the steady-state approximation, as follows. We assume that immediately after the enzyme, the substrates, and any optional modifiers (inhibitors and activators) are brought into contact, the reaction system passes through a relatively short transient phase. The amount of substrates consumed during the transient phase is assumed to be negligibly small compared to the total initial amount of substrates. We will further assume that during the subsequent steady-state phase of the enzyme reaction, the rate of change in the concentrations of all enzyme forms (enzyme complexes and the free enzyme) is negligibly small compared to the rate of change in the substrate and product concentrations.

2.2. Composition at steady state, allowing for "tight binding"

With the above assumptions and definitions, the full system of first-order ordinary differential equations, expressing the rate of change in species concentrations, can be written as shown in Eq. (4), where **S'** is the transpose of **S**, and the dot accent ($\dot{\mathbf{c}}$) represents first derivatives with respect to time. The steady-state condition is shown as Eq. (5), where the left-hand side is an n_S-vector. Eq. (5) represents a system of simultaneous nonlinear algebraic equations for the unknown concentrations of species at steady state.

$$\dot{\mathbf{c}} = \mathbf{S}'v \tag{4}$$

$$0 = \mathbf{S}'v \tag{5}$$

The system of nonlinear Eqs. (5) does not have a unique solution, because these equations are linearly dependent. We can remove this linear dependence by replacing the first n_E nonlinear equations by the mass balances for component species. Thus, the right-hand side of Eq. (5) can be partitioned as shown in Eq. (6).

$$0 = \begin{pmatrix} \mathbf{F}\tilde{\mathbf{c}} - \mathbf{c}^{(t)} \\ \mathbf{T}'\mathbf{v} \end{pmatrix} \tag{6}$$

Finally, the composition at steady-state can be computed by solving the mixed system of linear and nonlinear algebraic Eqs. (6) by an appropriate iterative method.
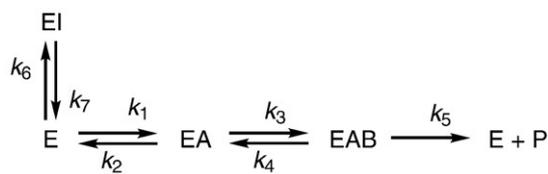
2.3. Initial rate law

The initial reaction rate can be expressed in terms of the steady-state concentrations of species as shown in Eq. (7), where p is the index of the first product appearing on the right-hand side the overall reaction. The observable initial rate of an enzyme reaction is defined by Eq. (8), where Δr is the difference molar response coefficient, and **r** in Eq. (9) is the vector of molar response coefficients (e.g., extinction coefficients in UV/Vis spectroscopy) for the reactants.

$$v \equiv \dot{c}_p = \sum_{i=1}^{n_R} S_{i,p} k_i \tilde{c}_p^{S_{i,p}} \tag{7}$$

$$v_{obs} = \Delta r \, v \tag{8}$$

$$\Delta r = \mathbf{s}'\mathbf{r} \tag{9}$$

It should be noted that the choice of specifically the first overall product (index p above) is arbitrary; any other product appearing on the right-hand side of the overall reaction would suffice, because the order in which either substrates or reaction products are written down in the overall reaction is also arbitrary. The above formalism is fully applicable to reversible reactions, because any

Scheme 1.

contribution of the reverse reaction would be appropriately captured by a negative term in the summation in Eq. (7).

2.4. Algorithmic implementation

The above procedure is now implemented in the DynaFit software package [4,5]. The program scans textual input representing an arbitrary reaction mechanism, and, in the process, automatically constructs the vectors and matrices $\mathbf{v}$, $\mathbf{s}$, $\mathbf{S}$, $\mathbf{T}$, and $\mathbf{F}$ defined above. Once these matrices are appropriately populated, the software then solves the nonlinear algebraic system (6) by using the multi-dimensional Newton–Raphson method [8, p. 379].

2.5. Illustrative example

Scheme 1 represents the simplest possible mechanism for protein kinase inhibition. The enzyme follows the "Ordered Sequential Bi Uni" catalytic mechanism [1], and the inhibitor binds only to the free enzyme. This reaction scheme implies that (a) the release of the first product is rate limiting, and (b) the experimental conditions are rendering the assay essentially irreversible. However, our general numerical formalism applies equally to any arbitrary mechanism.

To represent the steady-state initial rate problem corresponding to Scheme 1 in DynaFit, the input file contains the following text:

```
[task]
 data = rates
 approximation = steady−state
[reaction] | A + B −−−> P
[enzyme] | E
[modifiers] | I
[mechanism]
 E + A <===> E.A : k1 k2
 E.A + B <===> E.A.B : k3 k4
 E.A.B −−−−> E + P : k5
 E + I <===> E.I : k6 k7
```

When DynaFit scans the above text fragment, it automatically populates the stoichiometric matrix corresponding to Scheme 1, given by Eq. (10). Similarly, DynaFit automatically derives the truncated stoichiometric matrix, defined in Eq. (11); the formula matrix $\mathbf{F}$, shown in Eq. (12); and the stoichiometric vector for the overall reaction $A + B \rightarrow P$, Eq. (13). For clarity, all zero entries in the matrices below are represented by the dot symbol.

$$
\mathbf{S} = \begin{array}{c} \\ k_1 \\ k_2 \\ k_3 \\ k_4 \\ k_5 \\ k_6 \\ k_7 \end{array}
\begin{array}{c} A \\ \left(\begin{array}{c} -1 \\ +1 \\ \cdot \\ \cdot \\ \cdot \\ \cdot \\ \cdot \end{array} \right. \end{array}
\begin{array}{c} B \\ \cdot \\ \cdot \\ -1 \\ +1 \\ \cdot \\ \cdot \\ \cdot \end{array}
\begin{array}{c} P \\ \cdot \\ \cdot \\ \cdot \\ \cdot \\ +1 \\ \cdot \\ \cdot \end{array}
\begin{array}{c} I \\ \cdot \\ \cdot \\ \cdot \\ \cdot \\ \cdot \\ -1 \\ +1 \end{array}
\begin{array}{c} E \\ -1 \\ +1 \\ -1 \\ \cdot \\ +1 \\ -1 \\ +1 \end{array}
\begin{array}{c} EA \\ +1 \\ -1 \\ -1 \\ +1 \\ \cdot \\ \cdot \\ \cdot \end{array}
\begin{array}{c} EAB \\ \cdot \\ \cdot \\ +1 \\ -1 \\ -1 \\ \cdot \\ \cdot \end{array}
\begin{array}{c} EI \\ \cdot \\ \cdot \\ \cdot \\ \cdot \\ \cdot \\ +1 \\ +1 \end{array}
\left. \begin{array}{c} \\ \\ \\ \\ \\ \\ \\ \end{array} \right)
\tag{10}
$$

$$
\mathbf{T} = \begin{array}{c} \\ k_1 \\ k_2 \\ k_3 \\ k_4 \\ k_5 \\ k_6 \\ k_7 \end{array}
\begin{array}{c} EA \\ \left(\begin{array}{c} +1 \\ -1 \\ -1 \\ +1 \\ \cdot \\ \cdot \\ \cdot \end{array} \right. \end{array}
\begin{array}{c} EAB \\ \cdot \\ \cdot \\ +1 \\ -1 \\ -1 \\ \cdot \\ \cdot \end{array}
\begin{array}{c} EI \\ \cdot \\ \cdot \\ \cdot \\ \cdot \\ \cdot \\ +1 \\ -1 \end{array}
\left. \begin{array}{c} \\ \\ \\ \\ \\ \\ \\ \end{array} \right)
\tag{11}
$$

$$
\mathbf{F} = \begin{array}{c} E \\ A \\ B \\ P \\ I \end{array}
\begin{array}{c} E \\ \left(\begin{array}{c} 1 \\ \cdot \\ \cdot \\ \cdot \\ \cdot \end{array} \right. \end{array}
\begin{array}{c} A \\ \cdot \\ 1 \\ \cdot \\ \cdot \\ \cdot \end{array}
\begin{array}{c} B \\ \cdot \\ \cdot \\ 1 \\ \cdot \\ \cdot \end{array}
\begin{array}{c} P \\ \cdot \\ \cdot \\ \cdot \\ 1 \\ \cdot \end{array}
\begin{array}{c} I \\ \cdot \\ \cdot \\ \cdot \\ \cdot \\ 1 \end{array}
\begin{array}{c} EA \\ 1 \\ 1 \\ \cdot \\ \cdot \\ \cdot \end{array}
\begin{array}{c} EAB \\ 1 \\ 1 \\ 1 \\ \cdot \\ \cdot \end{array}
\begin{array}{c} EI \\ 1 \\ \cdot \\ \cdot \\ \cdot \\ 1 \end{array}
\left. \begin{array}{c} \\ \\ \\ \\ \end{array} \right)
\tag{12}
$$

$$
s = \begin{array}{cccccccc} A & B & P & I & E & EA & EAB & EI \\ (-1 & -1 & +1 & \cdot & \cdot & \cdot & \cdot & \cdot) \end{array}
\tag{13}
$$

The DynaFit software internally constructs the initial-rate model as follows. The vector of elementary rate terms is

$$
\mathbf{v} = \begin{pmatrix} k_1 & c_E & c_A \\ k_2 & c_{EA} & \\ k_3 & c_{EA} & c_B \\ k_4 & c_{EAB} & \\ k_5 & c_{EAB} & \\ k_6 & c_E & c_I \\ k_7 & c_{EI} & \end{pmatrix}.
\tag{14}
$$

The differential-equation system (Eq. (4)), internally derived by DynaFit, is defined by Eqs. (15–22). Please note that the right-hand sides of Eq. (15–22) are obtained simply as the matrix product $\mathbf{S'} \, \mathbf{v}$.

$$
\dot{c}_A = -k_1 \, c_E \, c_A + k_2 \, c_{EA}
\tag{15}
$$

$$
\dot{c}_B = -k_3 \, c_{EA} \, c_B + k_4 \, c_{EAB}
\tag{16}
$$

$$
\dot{c}_P = +k_5 \, c_{EAB}
\tag{17}
$$

$$
\dot{c}_I = -k_6 \, c_E \, c_I + k_7 \, c_{EI}
\tag{18}
$$

$$
\dot{c}_E = -k_1 \, c_E \, c_A + k_2 \, c_{EA} + k_5 \, c_{EAB} - k_6 \, c_E \, c_I + k_7 \, c_{EI}
\tag{19}
$$

$$
\dot{c}_{EA} = +k_1 \, c_E \, c_A - k_2 \, c_{EA} - k_3 \, c_{EAB} \, c_B + k_4 \, c_{EAB}
\tag{20}
$$

$$
\dot{c}_{EAB} = +k_3 \, c_{EA} \, c_B - (k_4 + k_5)c_{EAB}
\tag{21}
$$

$$
\dot{c}_{EI} = +k_6 \, c_E \, c_I - k_7 \, c_{EI}
\tag{22}
$$

The steady-state condition is obtained by setting all left-hand sides above to zero, which produces the system of simultaneous nonlinear algebraic (Eqs. (23–30)), where the concentrations at any arbitrary time c have been replaced by the steady-state concentrations $\bar{c}$. The nonlinear system (Eq. (23–30)) cannot have a unique solution, because of linear dependence among individual equations. For example, Eq. (26) is obtained simply by multiplying Eq. (30) by minus one.

$$
0 = -k_1 \, \tilde{c}_E \, \tilde{c}_A + k_2 \, \tilde{c}_{EA}
\tag{23}
$$

$$
0 = -k_3 \, \tilde{c}_{EA} \, \tilde{c}_B + k_4 \, \tilde{c}_{EAB}
\tag{24}
$$

$$
0 = +k_5 \, \tilde{c}_{EAB}
\tag{25}
$$

$$
0 = -k_6 \, \tilde{c}_E \, \tilde{c}_I + k_7 \, \tilde{c}_{EI}
\tag{26}
$$

$$0 = -k_1\, \tilde{c}_E\, \tilde{c}_A + k_2\, \tilde{c}_{EA} + k_5\, \tilde{c}_{EAB} - k_6\, \tilde{c}_E\, \tilde{c}_I + k_7\, \tilde{c}_{EI} \tag{27}$$

$$0 = +k_1\, \tilde{c}_E\, \tilde{c}_A - k_2\, \tilde{c}_{EA} - k_3\, \tilde{c}_{EAB}\, \tilde{c}_B + k_4\, \tilde{c}_{EAB} \tag{28}$$

$$0 = +k_3\, \tilde{c}_{EA}\, \tilde{c}_B - (k_4 + k_5)\, \tilde{c}_{EAB} \tag{29}$$

$$0 = +k_6\, \tilde{c}_E\, \tilde{c}_I - k_7\, \tilde{c}_{EI} \tag{30}$$

To remove this linear dependence, DynaFit replaces the first n_E nonlinear equations in the system (Eqs. (23–30)) by the mass balances for the component species, represented by the vector $F\tilde{c} - c^{(t)}$.

$$0 = \tilde{c}_A + \tilde{c}_{EA} + \tilde{c}_{EAB} - c_A^{(t)} \tag{31}$$

$$0 = \tilde{c}_B + \tilde{c}_{EAB} - c_B^{(t)} \tag{32}$$

$$0 = \tilde{c}_P - c_P^{(t)} \tag{33}$$

$$0 = \tilde{c}_I + \tilde{c}_{EI} - c_I^{(t)} \tag{34}$$

$$0 = \tilde{c}_E + \tilde{c}_{EA} + \tilde{c}_{EAB} + \tilde{c}_{EI} - c_E^{(t)} \tag{35}$$

The concentrations of all molecular species at steady state are then computed by iteratively solving the combined system of Eqs. (28–35), which corresponds to the general Eq. (6) above. The intrinsic initial rate is computed by applying the general formula (Eq. (7)), which, when applied to Scheme 1, turns into Eq. (36). Finally, the observable initial rate is computed by using Eq. (37).
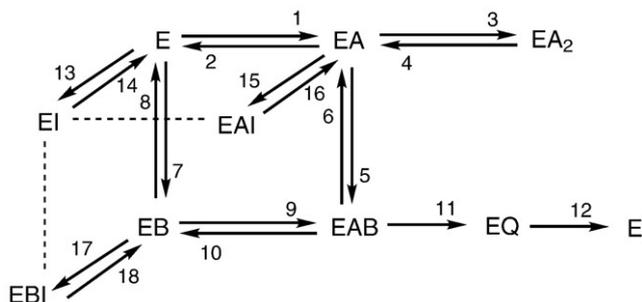
$$v = k_5\, \tilde{c}_{EAB} \tag{36}$$

$$v_{\text{obs}} = (r_P - r_A - r_B)v \tag{37}$$

All these manipulations and derivations are done within DynaFit completely transparently to the user; they are described here merely for illustration purposes. The only required input is the symbolic description of the system in the stoichiometric notation $E + A <===> E.A : k1\ k2$, etc.

3. Applications

In this section we give two examples illustrating the usefulness of the general numerical models for inhibition of protein kinases under the steady-state approximation.

Table 1
Numerical values of rate constants appearing in Scheme 2 that were used either in the algebraic model defined by Eqs. (38–57) or in a DynaFit numerical model defined by Eqs. (6–8) and the appropriate stoichiometric matrix.

k_1	0.1 $\mu M^{-1}\,s^{-1}$	k_2	10 s^{-1}
k_3	0.1 $\mu M^{-1}\,s^{-1}$	k_4	1000 s^{-1}
k_5	0.1 $\mu M^{-1}\,s^{-1}$	k_6	1 s^{-1}
k_7	0.1 $\mu M^{-1}\,s^{-1}$	k_8	100 s^{-1}
k_9	0.1 $\mu M^{-1}\,s^{-1}$	k_{10}	0.1 [a] s^{-1}
k_{11}	1000 s^{-1}	k_{12}	10 s^{-1}
k_{13}	1 $\mu M^{-1}\,s^{-1}$	k_{14}	0.01 s^{-1}
k_{15}	1 $\mu M^{-1}\,s^{-1}$	k_{16}	0.1 s^{-1}
k_{17}	1 $\mu M^{-1}\,s^{-1}$	k_{18}	0.1 s^{-1}

[a] Thermodynamic cycle: $k_{10} = k_2 k_6 k_7 k_9 / k_1 k_5 k_8$; see text.

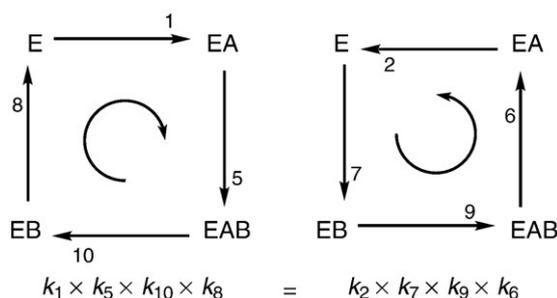### 3.1. Simulation study: inhibition of cAMP-dependent kinase by bisubstrate analog inhibitors

The main purpose of this heuristic simulation experiment is twofold. First, it verifies that our generalized matrix algorithm produces numerically correct results, by comparing the simulated initial rates with the traditional algebraic method (under the special conditions where the algebraic method is applicable). Secondly, the example illustrates the important general issue of thermodynamic cycles.

The reaction mechanism shown in Scheme 2 represents inhibition of cAMP-dependent kinase by a hypothetical bisubstrate analog inhibitor [9]. For clarity, only numerical indices of rate constants are shown (e.g., "1" stands for k_1). The approximate values of most rate constants k_1 through k_{18} were chosen on the basis of literature reports [9–12] (Table 1).

The inhibition mechanism shown in Scheme 2 brings up the important issue of thermodynamic cycles. Not all rate constants in Scheme 2 can have arbitrary values. Instead, one of eight rate constants in the cycle defined by species E–EA–EAB–EB–E must be defined in terms of the remaining seven constants, in order to satisfy the equality $k_1 k_5 k_8 k_{10} = k_2 k_6 k_7 k_9$ (see Scheme 3).

It may not be straightforward to decide which of the rate constants that appear in a thermodynamic cycle should be defined in terms of remaining rate constants. In the specific case of cAMP-dependent kinase, Kong and Cook [10] had independently measured the values of rate constants for both the association and the dissociation of MgATP (k_1, k_2), as well as the association and dissociation rate constants for a particular peptide substrate (k_7, k_8). The equilibrium dissociation constant k_6/k_5 has also been determined; in the case of Kemptide (LRRASLG) substrate, it is known that $k_6/k_5 = 200\ \mu M^1$ [12]. Based on these considerations, we have arbitrarily decided to express the rate constant k_{10} as $k_2 k_6 k_7 k_9 / k_1 k_5 k_8$.

The dotted lines in Scheme 2 represent additional binding and dissociation steps that could, in principle, be included in the mechanism. We have purposely not included them, in order to reduce the number of thermodynamic cycles. In polycyclic reaction mechanisms, the number of thermodynamic constraints quickly

Scheme 2.

$$k_1 \times k_5 \times k_{10} \times k_8 \qquad = \qquad k_2 \times k_7 \times k_9 \times k_6$$
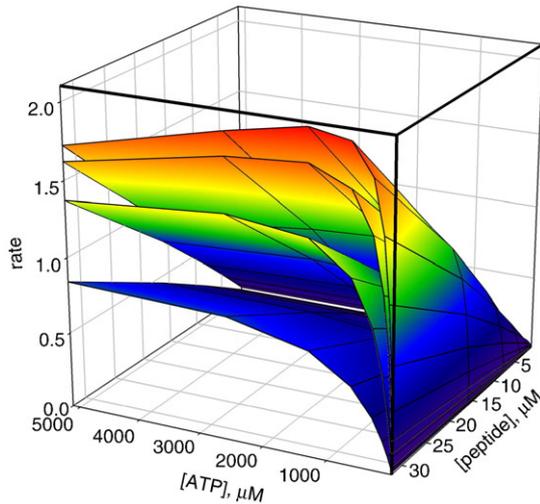
Scheme 3.

Fig. 1. Simulated inhibition of cAMP-dependent kinase inhibition by a bisustrate inhibitor, according to the mechanism shown in Scheme 2. All rate constants are given in Table 1. Initial rates were simulated either by using the algebraic Eqs. (38)–(57) or by using the numerical approach, Eqs. (6) and (8). The results were exactly identical.

proliferates. For example, if we explicitly included the reversible step $EI + A \rightleftharpoons EAI$, then *two* additional cycles would originate, the first being E–EI–EAI–EA–E, and the second (larger) cycle being E–EI–EAI–EA–EAB–EB–E.

The reaction mechanism in Scheme 2 was treated in two different ways. First, using the King–Altman method [1,13], we derived the algebraic steady-state rate equation, Eqs. (38)–(57), and used it to simulate initial reaction rates. (The King–Altman derivation was performed automatically by computer, using an online tool freely available at www.biokin.com/king-altman.)

$$v = N / D \tag{38}$$

$$N = n_1 c_A c_B^2 + n_2 c_A^2 c_B + n_3 c_A c_B \tag{39}$$

$$
\begin{aligned}
D = &\, d_1 c_B^2 c_I + d_2 c_A c_B c_I + d_3 c_A c_B^2 + d_4 c_A^2 c_I + d_5 c_A^2 c_B + d_6 c_A^3 \\
&+ d_7 c_B c_I + d_8 c_B^2 + d_9 c_A c_I + d_{10} c_A c_B + d_{11} c_A^2 + d_{12} c_I \\
&+ d_{13} c_B + d_{14} c_A + d_{15}
\end{aligned} \tag{40}
$$

$$n_1 = k_4 k_5 k_7 k_9 k_{11} k_{12} k_{14} k_{16} k_{18} \tag{41}$$

$$n_2 = k_1 k_4 k_5 k_9 k_{11} k_{12} k_{14} k_{16} k_{18} \tag{42}$$

$$n_3 = (k_1 k_5 k_8 + k_2 k_7 k_9) k_4 k_{11} k_{12} k_{14} k_{16} k_{18} \tag{43}$$

$$d_1 = k_4 k_5 k_7 k_{12} k_{14} k_{16} k_{17} (k_{10} + k_{11}) \tag{44}$$

$$d_2 = (k_5 k_9 k_{11} k_{13} k_{16} k_{18} + k_{16} k_7 k_9 k_{14} k_{15} k_{18} + k_1 k_5 k_{10} k_{14} k_{16} k_{17}) k_{12} k_4 \tag{45}$$

$$d_3 = k_4 k_5 k_7 k_9 k_{14} k_{16} k_{18} (k_{11} + k_{12}) \tag{46}$$

$$d_4 = k_1 k_4 k_9 k_{12} k_{14} k_{15} k_{18} (k_6 + k_{11}) \tag{47}$$

$$d_5 = [k_3 k_6 k_7 k_{12} + k_1 k_4 k_5 (k_{11} + k_{12})] k_9 k_{14} k_{16} k_{18} \tag{48}$$

$$d_6 = k_1 k_3 k_9 k_{12} k_{14} k_{16} k_{18} (k_6 + k_{11}) \tag{49}$$

$$
\begin{aligned}
d_7 = &\, k_4 k_5 k_8 k_{12} k_{13} k_{16} k_{18} (k_{10} + k_{11}) \\
&+ k_2 k_4 k_7 k_{12} k_{14} k_{16} k_{17} (k_6 + k_{10} + k_{11})
\end{aligned} \tag{50}
$$

$$d_8 = k_4 k_5 k_7 k_{12} k_{14} k_{16} k_{18} (k_{10} + k_{11}) \tag{51}$$

$$
\begin{aligned}
d_9 = &\, k_2 k_4 k_9 k_{12} k_{13} k_{16} k_{18} (k_6 + k_{11}) \\
&+ k_1 k_4 k_8 k_{12} k_{14} k_{15} k_{18} (k_6 + k_{10} + k_{11})
\end{aligned} \tag{52}
$$

$$
\begin{aligned}
d_{10} = &\, (k_5 k_9 k_{11} k_{12} + k_6 k_7 k_9 k_{12} + k_1 k_5 k_8 k_{12} + k_2 k_7 k_9 k_{12} \\
&+ k_1 k_5 k_{10} k_{12} + k_1 k_5 k_8 k_{11} + k_2 k_7 k_9 k_{11}) k_4 k_{14} k_{16} k_{18}
\end{aligned}
$$

$$d_{11} = [k_4 k_9 (k_6 + k_{11}) + k_3 k_8 (k_6 + k_{10} + k_{11})] k_1 k_{12} k_{14} k_{16} k_{18} \tag{53}$$

$$d_{12} = (k_6 + k_{10} + k_{11}) k_2 k_4 k_8 k_{12} k_{13} k_{16} k_{18} \tag{54}$$

$$d_{13} = [k_5 k_8 (k_{10} + k_{11}) + k_2 k_7 (k_6 + k_{10} + k_{11})] k_4 k_{12} k_{14} k_{16} k_{18} \tag{55}$$

$$d_{14} = [k_2 k_9 (k_6 + k_{11}) + k_1 k_8 (k_6 + k_{10} + k_{11})] k_4 k_{12} k_{14} k_{16} k_{18} \tag{56}$$

$$d_{15} = (k_6 + k_{10} + k_{11}) k_2 k_4 k_8 k_{12} k_{14} k_{16} k_{18} \tag{57}$$

We then compared the numerical results with the output from our newly proposed general algorithm. To make the two methods sufficiently comparable, and to satisfy the more stringent requirements of the algebraic method, we chose a particular value for the enzyme concentration that is 10^6 times lower than the concentrations of substrates, and of the inhibitor. The simulated initial rates are shown in Fig. 1. Regardless of which mathematical model was used (algebraic or numerical), the results were identical within eight significant digits.

These results empirically demonstrate the validity of the general numerical model defined by Eqs. (6) and (8). However, the general numerical method is extensible to "tight binding" inhibition [2] without any restrictions on the stoichiometry of enzyme–inhibitor complexes, whereas the classic algebraic method can only be applied to weakly bound inhibitors.

Most importantly, the algebraic model defined by Eqs. (38–57) is very complex. Entering these algebraic equations into a conventional data-fitting program would be a tedious and error prone procedure. In contrast, the same kinetic model would be defined in the DynaFit software by entering a few easily understandable biochemical equations, which are listed under Scheme 2.

3.2. Experimental study: inhibition of p56lck tyrosine kinase

Faltynek et al. [14] reported that the quinolone heterocycle WIN61651 is a mixed-type noncompetitive (with respect to peptide substrates) inhibitor of the *p56*lck tyrosine kinase. Fig. 2 shows the raw

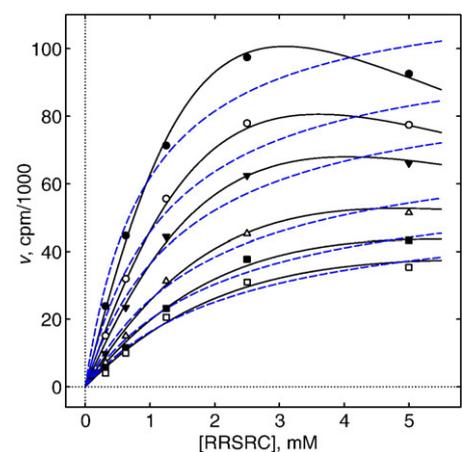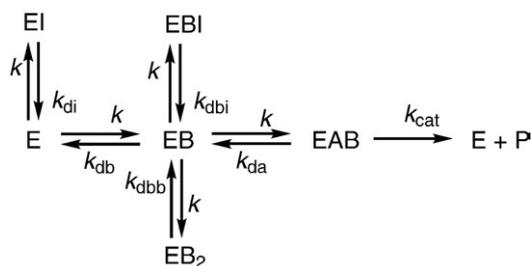**Fig. 2.** Inhibition of *p56*lck kinase by WIN61651-Peptide binding site. Raw experimental data were extracted from a previously published report [14]. The kinase was preincubated at various concentrations of the peptide substrate RRSRC, either in the absence of inhibitor (top curve) or in the presence of 20, 40, 60, 80 μM WIN61651 (curves from top to bottom). The reaction was started by the addition of 600 μM [γ32-P] ATP. Incorporation of $^{32}PO_4$ into RRSRC (*cpm*, counts per minute) was measured as described elsewhere [15]. The raw data were fit either to the noncompetitive algebraic model represented by Eq. (58) (thin dashed curves), or to a more complex steady-state model represented by Scheme 4 (thick solid curves).

Scheme 4.

experimental data from a kinetic study, in which the ATP concentration was held constant and the substrate (RRSRC) was varied. The authors used the algebraic Eq. (58) to perform the least-squares fit of the experimental data. The best least-squares fit to the algebraic model is shown as thin dashed curves in Fig. 2. The published best-fit values of inhibition constants were $K_{is} = (18.3 \pm 4.3)$ μM (binding of inhibitor to the free enzyme) and $K_{ii} = (67.0 \pm 17.9)$ μM (binding of inhibitor to the kinase-ATP complex).

$$v = V_{max} \frac{c_s}{c_s(1 + c_I / K_{ii}) + K_m(1 + c_I / K_{is})} \qquad (58)$$

The dashed "best-fit" model curves in Fig. 2, which correspond to the algebraic model for noncompetitive inhibition (Eq. (58)) clearly do not describe the experimental data sufficiently well. Note that at very high substrate concentrations, the observed enzymatic activity is decreasing (substrate inhibition), which is not captured by the fitting model. We have recently reported [16] that ignoring substrate inhibition can lead to erroneous conclusions regarding the inhibition mechanism. Specifically, a particular inhibitor appeared "competitive" when substrate inhibition was ignored. However, once substrate inhibition was properly taken into account, it became clear that the inhibition mechanism is mixed-type noncompetitive.

A kinetic model that better describes the published $p56^{lck}$ inhibition data is shown in Scheme 4. The originally published kinetic model [14] contained four adjustable model parameters, namely, V_{max}, K_m, K_{is}, and K_{ii} in Eq. (58). These kinetic constants correspond to the microscopic rate constants k_{cat}, k_{db}, k_{di}, and k_{dbi}, respectively, in Scheme 4. However, in Scheme 4 we have introduced an additional adjustable parameter, the dissociation rate constant k_{dbb}. This corresponds to the ternary complex EB_2, in which the peptide substrate is bound not only in the active site, but also in an allosteric site. The bimolecular association rate constant k was assumed to be identical for all steps in the postulated mechanism.

The substrate-inhibition mechanism in Scheme 4 was represented in DynaFit as shown in the Appendix. The best-fit values of microscopic rate constants characterizing the inhibition steps were $k_{di} = (28 \pm 2)s^{-1}$ and $k_{dbi} = (2.6 \pm 11)s^{-1}$. The corresponding equilibrium dissociation constants are $k_{is} = k_{di}/k = 28$ μM and $k_{ii} = k_{dbi}/k = 2.6$ μM. These results are consistent with the possibility that the binding of WIN61651 to the free enzyme is very much weaker when compared with the binding to the enzyme–peptide complex. This is the opposite of what the original report [14] suggested ($K_{is} = 18$ μM, $K_{ii} = 67$ μM).

4. Discussion

The main purpose of the example problem given above, discussing the inhibition of $p56^{lck}$ tyrosine kinase, was *not* to

suggest the "true" or "improved" mechanism inhibition in this particular case—even though it is clear that the solid curves in Fig. 2 (generated from the newly proposed numerical model) fit the experimental data very much better than what was seen in the original report [14]. Rather, the main purpose of the example problem was to illustrate a general *method* of kinetic analysis, which could be used to determine a more plausible inhibition mechanism without the use traditional closed-form algebraic rate equations.

Instead of a single algebraic equation for steady-state initial rates, here we rely on a complete system of simultaneous nonlinear algebraic equations, Eq. (6), which are solved numerically (iteratively), by using the multidimensional Newton–Raphson method [8]. The general form of these simultaneous nonlinear equations allows our numerical formalism to be employed even when the concentration of the enzyme is not negligibly small, when compared to the concentrations of all substrates and modifiers (inhibitors and activators). Thus, the numerical method is more generally applicable than the conventional algebraic formalism for steady-state initial rate kinetics [1].

The method proposed here is fully applicable to "tight binding" enzyme inhibitors [2] without any restrictions being placed on the stoichiometry of inhibitor binding, or on any other aspect of the inhibition mechanism. Being able to properly analyze the kinetic of "tight binding" inhibition has great practical value, because most therapeutic enzyme inhibitors are "tight binding" under the conditions of typical *in vitro* assays. Thus far, a fully general treatment of initial reaction rates in enzyme assays involving "tight binding" inhibitors had been possible under the relatively restrictive rapid-equilibrium approximation [3]. However, literature reports (see, for example, ref. [6]) convincingly demonstrate that ADP release could be rate-limiting and, therefore, the steady-state approximation is more suitable than the rapid-equilibrium approximation.

In the specific example of the $p56^{lck}$ kinase, we can only speculate why the authors of the original report [14] chose to ignore the obvious mismatch between the experimental data (symbols in Fig. 2) and the "best-fit" algebraic model (dashed curves). Perhaps the authors were somewhat discouraged by the prospect of having to derive appropriate algebraic rate equations. Experience shows that many practicing enzymologists find the exercise of algebraic derivations very daunting, and a mathematically minded specialist might not always be a member of the team. What is worse, if the kinase inhibitor is "tight binding" [2], an algebraic model might not even exist as a matter of principle.

The method proposed in this paper allows the computer to automatically construct the appropriate mathematical model for enzymatic initial rates, under the steady-state approximation, arising from an arbitrary reaction mechanism. The investigator needs to provide only the symbolic definition of the reaction mechanism, in the usual language of stoichiometric equations. For example, to introduce the "substrate inhibition" step in the case of $p56^{lck}$ tyrosine kinase, one can enter the text E.B + B <==> E.B.B to represent the (non-productive) binding of a second substrate molecule to the catalytically active enzyme–substrate complex. The DynaFit software "understands" this notation, and updates the underlying mathematical model accordingly.

It is legitimate to ask why it is still useful to keep the steady-state approximation during numerical calculations, instead of the simulation of the full set of differential equations, without any limitations at all. A practical usefulness of the steady-state approach stems from the fact that, in the completely general approach, the investigator would be compelled to arbitrarily select some particular point in time at which the "initial rate" should be computed (as the first derivative of the observable physical quantity with respect to time). Selecting this "initial" point in

Table 2
Numerical data for the inhibition of $p56^{lck}$ tyrosine kinase by a quinolone inhibitor extracted by image-digitization from ref. [14].

[B], mM	[I], μM					
	0	10	20	40	60	80
0.3125	24	15	10	7	6	4
0.625	45	32	23	15	12	10
1.25	71	56	44	31	23	21
2.5	97	78	62	45	38	31
5	93	77	66	51	43	35

time is not simple, because in the fully general approach (based on numerical integration) the instantaneous reaction velocity is changing essentially at all reaction times.

The generalized numerical method described in this paper requires two important caveats. The first limitation has to do with the steady-state approximation not necessarily being satisfied at extremely low concentrations of reactants.

As was stated in the Theory, we assume that when the enzyme and the substrates are mixed, the system relatively quickly passes through a transient phase and, subsequently, reaches a *bona fide* steady-state phase. The "initial" reaction rates computed by the present algorithm pertain this putative steady-state phase. However, if the substrate concentrations in an actual experiment were extremely low (comparable in magnitude with the enzyme concentration), a genuine steady state would never be reached. Under these extreme circumstances, a significant proportion of the substrates would be consumed before a "steady-state" composition could be attained. This limitation of the present method does not affect the analysis of practically available *in vitro* kinetic data. For practical reasons, the substrate concentrations in initial-rate experiments typically are very much higher than the concentrations of the enzyme.

The second limitation of the present method lies in that the investigator must explicitly define any thermodynamic cycles, which cause algebraic dependencies among microscopic rate constants (e.g., $k_{10} = k_2 k_6 k_7 k_9 / k_1 k_5 k_8$ in Scheme 2). This logistical chore is also present in the traditional algebraic approach, where it manifests in the form of the Haldane equations [1]. Future implementations of the steady-state initial rate method in the DynaFit software package will identify the presence of thermodynamic cycles, if any are present, and suggest a complete list of choices to express the algebraic dependencies.

With these caveats and warnings kept firmly in mind, it is hoped that the convenience and the full generality of the symbolic approach to steady-state kinetic modeling will be useful to researchers active in protein kinase research.

Acknowledgements

Appendix

The following DynaFit [4] script will fit the experimental data shown in Table 2 to the inhibition mechanism shown in Scheme 4. All units used are micromoles per liter and seconds. The bimolecular association rate constant k was assumed identical for all steps ($k = 1$ μM^{-1} s^{-1}). The dissociation rate constant for ATP (step EA-$B{\to}EB + A$) was fixed at $k_{dab} = 140$ s^{-1}, approximately corresponding

to $K_m = 140$ μM experimentally determined for ATP [14]. All other rate constants were optimized in the regression.

```
[task]
  task  =  fit
  data  =  rates
  approx  =  steady−state
  model  =  allosteric substrate inhibition
[reaction] | A  +  B  −−−>  P
[enzyme] | E
[modifiers] | I
[responses] | difference  =  1000000
[concentrations] | E  =  0.001,  A  =  600
[mechanism]
  E  +  B  <===>  E.B  :  k kdb
  E.B  +  A  <===>  E.B.A  :  k kda
  E.B  +  B  <===>  E.B.B  :  k kdbb
  E.B.A  −−−>  E  +  P  :  kcat
  E  +  I  <===>  E.I  :  k kdi
  E.B  +  I  <===>  E.B.I  :  k kdbi
[constants]
  k  =  1,  kda  =  140,  kcat  =  1 ?
  kdb  =  1000 ?,  kdbb  =  1000 ?
  kdi  =  10 ?,  kdbi  =  10 ?
[data]
  directory ./p56lck/data
  extension txt
  variable B
file i00 | concentration I  =  0
file i10 | concentration I  =  10
file i20 | concentration I  =  20
file i40 | concentration I  =  40
file i60 | concentration I  =  60
file i80 | concentration I  =  80
[output]
  directory ./p56lck/output
[end]
```

References

[1] I.H. Segel, Enzyme Kinetics, Wiley, New York, 1975.
[2] S. Szedlacsek, R.G. Duggleby, Kinetics of slow and tight-binding inhibitors, Meth. Enzymol. 249 (1995) 144–180.
[3] P. Kuzmič, A generalized numerical approach to rapid-equilibrium enzyme kinetics, Application to 17_-HSD, Mol. Cell. Endocrinol. 248 (2006) 172–181.
[4] P. Kuzmič, Program DYNAFIT for the analysis of enzyme kinetic data: application to HIV proteinase, Anal. Biochem. 237 (1996) 260–273.
[5] P. Kuzmič, DynaFit - a software package for enzymology, Meth. Enzymol. 467 (2009) 247–280.
[6] M.M. Keshwani, T.K. Harris, Kinetic mechanism of fully activated S6K1 protein kinase, J. Biol. Chem. 283 (2008) 11972–11980.
[7] W.R. Smith, R.W. Missen, Chemical Reaction Equilibrium Analysis, John Wiley, New York, 1982.
[8] W.H. Press, B.P. Flannery, S.A. Teukolsky, W.T. Vetterling, Numerical Recipes in C: The Art of Scientific Computing, Cambridge University Press, Cambridge, 1992.
[9] A. Kuznetsov, A. Uri, G. Raidaru, J. Järv, Kinetic analysis of inhibition of cAMP-dependent protein kinase catalytic subunit by the peptidenucleoside conjugate AdcAhxArg6, Bioorg. Chem. 32 (2004) 527–535.
[10] C.T. Kong, P.F. Cook, Isotope partitioning in the adenosine 3′,5′-monophosphate dependent protein kinase reaction indicates a steady-state random kinetic mechanism, Biochemistry 27 (1988) 4795–4799.
[11] B.D. Grant, J.A. Adams, Pre-steady-state kinetic analysis of cAMP-dependent protein kinase using rapid quench flow techniques, Biochemistry 35 (1996) 2022–2029.
[12] J. Zhou, J.A. Adams, Participation of ADP dissociation in the rate determining step in cAMP-dependent protein kinase, Biochemistry 36 (1997) 15733–15738.
[13] E.L. King, C. Altman, A schematic method of deriving the rate laws for enzyme-catalyzed reactions, J. Phys. Chem. 60 (1956) 1375–1378.
[14] C.R. Faltynek, S. Wang, D. Miller, P. Mauvais, B. Gauvin, J. Reid, W. Xie, S. Hoekstra, P. Juniewicz, J. Sarup, R. Lehr, D.G. Sawutz, D. Murphy, Inhibition of lymphocyte activation by novel $p56^{lck}$ tyrosine kinase inhibitor, J. Enz. Inhib. 9 (1995) 111–122.
[15] S. Wang, R. Lehr, P. Stevis, X.M. Wang, J. Trevillyan, C.R. Faltynek, $p56^{lck}$ Interactions accelerate autophosphorylation and enhance activity toward exogenous substrates, Arch. Biochem. Biophys. 315 (1994) 60–67.
[16] P. Kuzmič, L. Cregar, S.Z. Millis, M. Goldman, Mixed-type noncompetitive inhibition of anthrax lethal factor protease by aminoglycosides, FEBS J. 273 (2006) 30543062.